JGR Space Physics

RESEARCH ARTICLE
10.1029/2019JA026760

On the Momentum Transfer From Polar to Equatorial Ionosphere

Jiannan Tu[1] **and Paul Song**[1,2]

[1]Space Science Laboratory, University of Massachusetts Lowell, Lowell, MA, USA, [2]Department of Physics and Applied Physics, University of Massachusetts Lowell, Lowell, MA, USA

Key Points:
- A multifluid-collisional-Hall MHD simulation model for simulating dynamics of magnetosphere-ionosphere-thermosphere coupling is developed
- Coupling within the entire magnetosphere-ionosphere system is through magnetohydrodynamic waves
- Prompt momentum transfer from polar to equatorial latitude ionosphere is established by fast magnetosonic waves

Supporting Information:
- Supporting Information S1

Correspondence to:
J. Tu,
Jiannan_Tu@uml.edu

Citation:
Tu, J., & Song, P. (2019). On the momentum transfer from polar to equatorial ionosphere. *Journal of Geophysical Research: Space Physics*, *124*. https://doi.org/10.1029/2019JA026760

Received 25 MAR 2019
Accepted 17 JUN 2019
Accepted article online 4 JUL 2019

Abstract During space weather events, a large amount of energy and momentum from the solar wind inputs into the ionosphere-thermosphere. A critical question is that if the solar wind-magnetosphere interaction drives only the open field region in the polar caps, how the solar wind energy and momentum are transmitted to the low latitude and equatorial ionosphere. This important issue has been studied over decades and is still poorly understood, impeding space weather forecasting ability. Here we use our newly developed 2.5-D ionosphere-thermosphere simulation model that self-consistently solves the density, velocity, and temperature for electrons, multiple ion and neutral species, and electromagnetic fields to study this challenging problem. The focus of the present study is on the prompt response of the ionosphere to a convection disturbance from the polar magnetosphere. The longer time scale responses caused by the neutral winds from the polar caps will be the topic of future studies. We show that the momentum is transferred from polar to equatorial ionosphere predominately by fast magnetosonic waves, and propagation of perturbations from the source region experiences delay, damping, and substantial reflection, and the ionosphere/thermosphere behaves like a low-band-pass filter. The finding from this study sheds new insight onto coupling processes within the magnetosphere-ionosphere system.

1. Introduction

Disturbances in the ionosphere-thermosphere can be caused by the solar wind-magnetosphere-ionosphere coupling and coupling within the ionosphere-thermosphere system. Such disturbances produce complex space weather phenomena (Buonsanto, 1999; Robinson & Behnke, 2001) that have severe impacts on the modern technology systems (e.g., Hapgood, 2012). On the other hand, the magnetosphere dynamics is significantly affected by the feedback of ionosphere, such as cold ionospheric ion outflow and the transport of cold-dense ions to the dayside magnetopause reconnection sites (Brambles et al., 2011; Walsh et al., 2014). The magnetosphere and ionosphere/thermosphere behave as a coherently coupled system (Borovsky, 2014). A prominent feature in this coupling process is the prompt response of the global ionospheric perturbations, which often show features correlated with those in the solar wind during the magnetically disturbed times. A typical example is that the upward flow in the dayside equatorial ionosphere responds in accordance with the solar wind and/or interplanetary magnetic field (IMF) changes (Fejer, 2011; Huang et al., 2005; Kelley et al., 2003).

It is commonly believed that for the southward IMF the solar wind momentum is transferred to the polar ionosphere, producing antisunward convection in the polar caps (e.g., Dungey, 1961). The fundamental question is what causes the dayside equatorial ionosphere to move when a driver is added in the polar region. Associated with this process is the transfer of momentum and energy from the polar region to the equator. We focus on the plasma velocity that is proportional to the linear momentum or the kinetic energy in this study. Some models assume that a prompt penetration electric field is the driver of global dayside ionosphere during the magnetic storms (Buonsanto, 1999; Fejer, 2011; Kelley et al., 2003). There are also studies showing that the electric field is a consequence of the plasma flow rather than the driver of plasma motion (Parker, 2007; Tu et al., 2008; Vasyliūnas, 2001). The energy and momentum in the solar wind is primarily transferred by reconnection at the magnetopause (Dungey, 1961) to the polar ionosphere via Alfvén waves (e.g., Song et al., 2009; Tu et al., 2014; Vasyliūnas, 2007; Wright, 1996, and references therein). The underlying physical mechanisms of the energy and momentum transfer from the polar latitude to equatorial ionosphere are, however, not well understood. Without clear understanding of the coupling mechanism one cannot estimate coupling efficiency and hence the magnitude of equatorial perturbations.

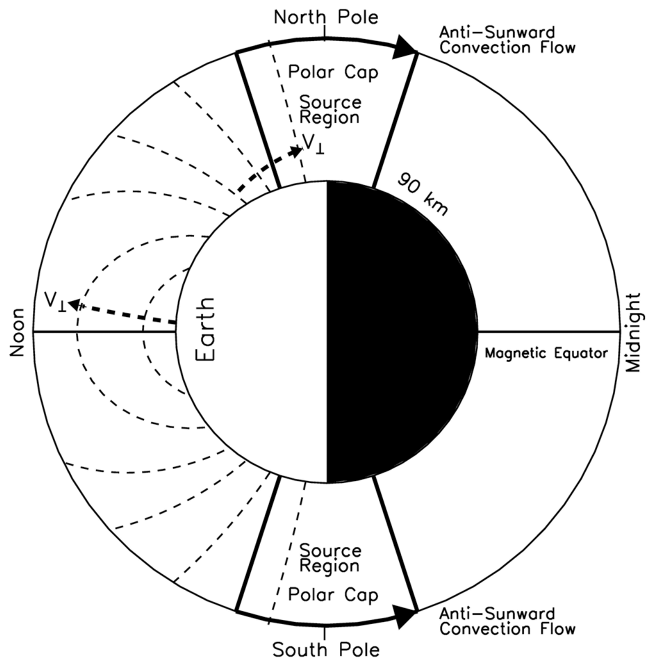

Figure 1. Schematic display of simulation domain within the noon-midnight magnetic meridian (not in scale). In the present study lower and upper boundaries are at altitude of 90 and 2,000 km, respectively. Several dipole magnetic field lines are plotted as dashed lines on the dayside. Dashed arrows schematically show ion bulk velocity component $V_\perp$ within the noon-midnight magnetic meridian and perpendicular to the background magnetic field.

A possible mechanism for the high-latitude to low-latitude ionospheric coupling is propagation of magnetohydrodynamic (MHD) waves that can carry significant momentum as suggested and discussed theoretically in, for example, Patel and Lagos (1985) and Song and Vasyliūnas (2014). Existence of fast magnetosonic waves propagating in the ionosphere has been shown by theoretical analysis (Kivelson, 2006; Kivelson & Southwood, 1988) and observations (e.g., Regi et al., 2014; Ziesolleck & Chamalaun, 1993). Evaluating coupling mechanisms has been extremely challenging because the (ionized) ionosphere and (neutral) thermosphere are collocated in a region with strong background magnetic field. The densities and temperatures of multiple species involved in this process change by several orders of magnitude within less than 2,000-km altitude. Existing models had to make substantial approximations, for example, steady state of the magnetic field as summarized in Richmond et al. (2014), which essentially removes the MHD waves from the solutions, or allowing only one-dimensional spatial variation (either along the magnetic field or in the vertical direction), which cannot describe a process that needs at least two dimensions. The coupling from polar to equatorial region needs at least two dimensions to describe, that is, the gradients in altitude direction at the same time allowing waves to propagate horizontally from the polar region to equator.

Besides MHD waves, hydromagnetic wave propagation in the ionosphere has also been extensively studied. Associated with hydromagnetic wave propagation in the ionosphere is the Afvén resonator phenomenon (e.g., Fraser, 1975; Fujita & Tamao, 1988; Kim et al., 2010; Lysak, 1993; Polyakov & Rapoport, 1981). It is thought that hydromagnetic waves in the frequency range about 0.2–10 Hz are guided in a duct between E region and about 400 km. The ionosphere is prescribed as a conducting media; the plasma dynamics is not explicitly included; that is, the plasma does not move as well as the density and pressure of the plasma do not change. The neutral dynamics is not considered either. Compared to solutions from MHD equations, the solution with a prescribed ionosphere is not able to self-consistently investigate coupling processes. The Alfvén resonator process, if existing, is naturally included in our simulation since the propagation of the MHD waves is self-consistently solved with plasma and neutral dynamics. It should be noted that the MHD waves actually are distinct from the hydromagnetic waves because the MHD waves involve plasma dynamics while the hydromagnetic waves do not.

Furthermore, transverse TM mode waves propagating in the ionosphere-Earth waveguide has been proposed as the electric field transmission mechanism and as the driver of equatorial ionosphere motion (Kikuchi et al., 1978) This mechanism is debatable because (1) the electromagnetic momentum of a vacuum wave is several orders of magnitude smaller than that required to drive ionosphere motion as will be discussed later and (2) instant arrival of the signals predicted by that theory contradicts to some observations that show apparent delays (e.g., Chi et al., 2001).

In this study we present simulation results from a new and unique 2.5-D (spatial variation in 2-D and three components vector variables) ionosphere-thermosphere simulation model (Tu & Song, 2016) that includes Ampere's and Faraday's laws in the governing equations, instead of the electrostatic electric field assumption used in all global ionosphere models, to provide numerical simulation evidence for the momentum transfer from polar latitudes to the equator and from high to low altitudes through MHD waves. This finding greatly elucidates the coupling process among different regions of the ionosphere during the prompt response phase. The modeling method is also applicable to partially ionized collisional gases around a star or other planets.

2. Simulation Method

The simulation is conducted for the noon-midnight magnetic meridian using our 2.5-D multifluid-collisional-Hall MHD simulation model with interspecies collisions. The model solves self-consistently

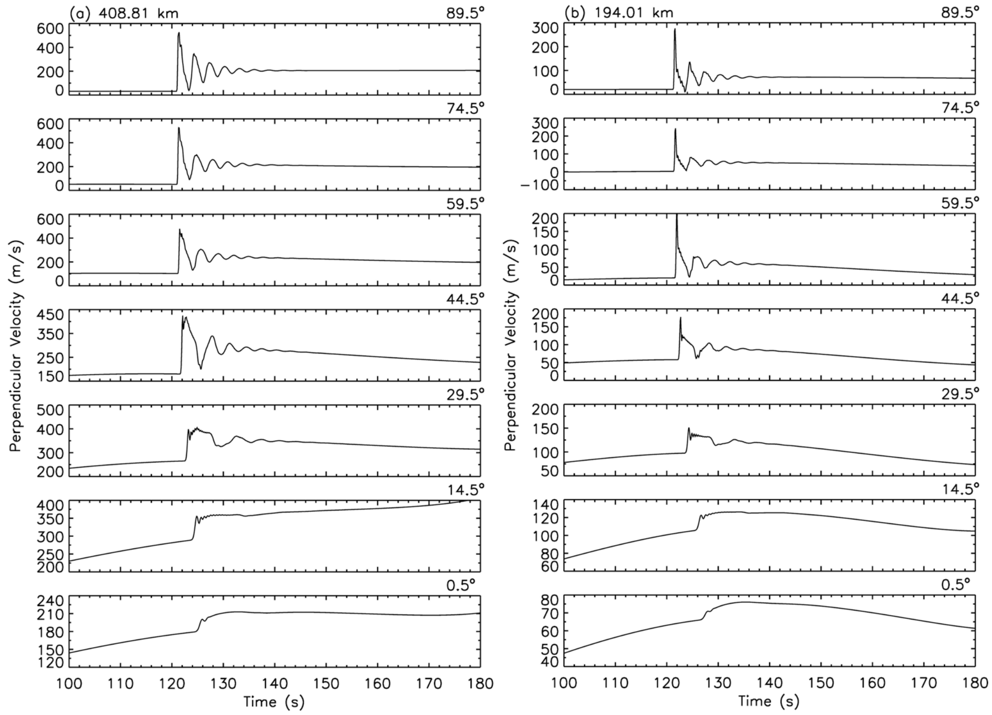

Figure 2. Panels (a) and (b) display time variation of $V_\perp$ for several magnetic latitudes at 408.81 and 194.01 km, respectively. Positive values represent poleward (at high and middle latitudes) or upward (at low and equatorial latitudes) velocities for the background dipole magnetic field used in the simulation. The simulation covers whole noon-midnight meridian plane while only the results for dayside Northern Hemisphere are shown.

time-dependent continuity, momentum, and energy equations for multiple ion and neutral species with photochemistry, plus generalized Ohm's law and Maxwell's equations. We use five-moment transport equations described in Schunk and Nagy (2000) for multiple ion species, with heat flow added in the energy equation of each individual species. The key point is that the inertial term is retained in the ion and neutral momentum equations and Faraday's law is solved. We implement an implicit difference scheme in cylindrical coordinates to numerically solve above governing equations with a time step of 0.01 s (see Tu & Song, 2016, for a detailed discussion of the model). The present simulation was conducted within the noon-midnight magnetic meridian. Figure 1 is a schematic display of the simulation domain and simulation setting for the present study. The magnetospheric driver is an antisunward flow applied to the top boundary (at 2,000-km altitude in the present simulation) for latitudes above 74° (assuming that polar latitudes are above 74° in this study) in both hemispheres. The upper boundary is flexible and can be set at the magnetopause or deep in the magnetotail. The open boundary conditions are used at remaining part of the top boundary at 2,000 km and the lower boundary at 90-km altitude. Because of strong ion-neutral collisions, the velocity and electric field perturbations basically do not penetrate significantly to the altitude below 150 km (see later in Figures 3 and 4), the lower boundary conditions are not important to the hydromagnetic wave energy deposition (Kivelson & Southwood, 1988). Two different lower boundary conditions have been tested: perturbation magnetic field $\delta\mathbf{B} = 0$ and $\partial\delta\mathbf{B}/\partial r = 0$, where r is radial distance. The simulation results from two lower boundary conditions are essentially the same with negligible quantitative difference. Note that the electric field is a derived quantity (through generalized Ohm's law resulting from electron momentum equation with electron inertia ignored), it is not necessary to specify boundary conditions for electric field.

The simulation started with initial distribution of the ionosphere and thermosphere originally based on Mass Spectrometer Incoherent Scatter and International Reference Ionosphere empirical models (Bilitza et al., 2017; Picone et al., 2002), which is obviously not in steady state and results in ion and electron flows as well as neutral winds. After simulating half an hour evolution of the system, the flow is substantially reduced with gradual evolving residual motion. This state of the ions and neutrals is used as the condition at $t = 0$. The antisunward flow is 200 m/s in value for the first 2 min and then is increased to 2,000 m/s within 0.5 s,

10.1029/2019JA026760

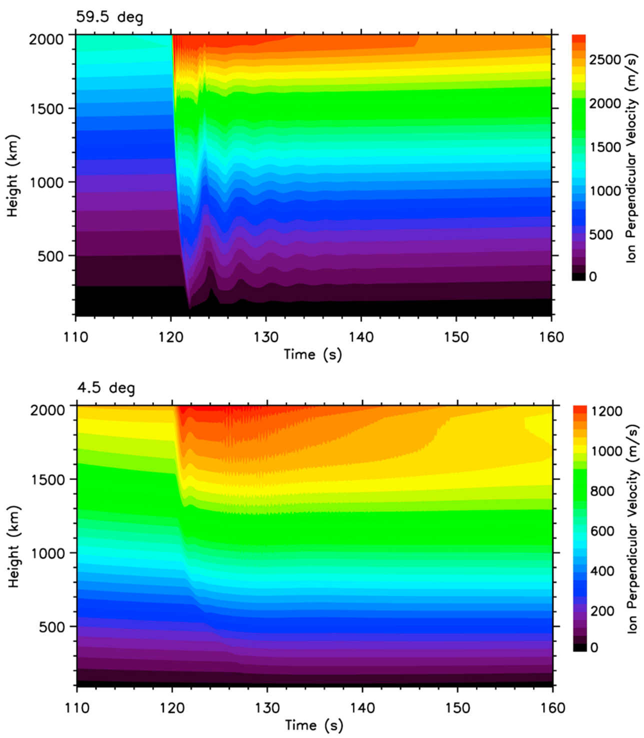

Figure 3. Ion bulk velocity component within the noon-midnight magnetic meridian and perpendicular to the background magnetic field as a function of time and height. The upper panel for magnetic latitude of 59.5° and bottom panel for 4.5°. On the dayside increase of the velocity perturbations is delayed in lower altitudes. The oscillation frequency of the velocity perturbations is higher at higher latitudes, showing that the ionosphere is a low-pass filter to the magnetohydrodynamic wave propagation. The color scale of two panels is different in order to better display features.

keeping that value later on, to simulate an ideal setting for solar wind-magnetosphere-ionosphere-thermosphere coupling in the case of a southward turning of the IMF. Note that the driver used in the present simulation is essentially a step function. We focus on the dayside ionosphere response to the open-magnetosphere motion that is driven by the solar wind and investigate how the plasma motion, or equivalently the momentum, propagates (with reflection) from the polar cap top boundary to lower latitudes and lower altitudes. As a diagnostics, the ionospheric response is represented with the time variation of the ion bulk velocity defined as $\mathbf{v} = \sum_s n_s \mathbf{v}_s / \sum_s n_s$, where n_s and $\mathbf{v}_s$ are the mass density and velocity, respectively, of the ion species s. In this simulation run, we include 5 ion (O^+, H^+, O_2^+, N_2^+, and NO^+) and 6 (O, H, O_2, N_2, NO, and N) neutral dominant ionosphere and thermosphere species plus electron species, a total of 12 fluids.

3. Results

Figure 2 shows the ion bulk velocity component that is within the noon-midnight magnetic meridian (simulation domain) and perpendicular to the background magnetic field at several magnetic latitudes for the altitudes of 408.81 and 194.01 km, respectively, in the dayside Northern Hemisphere. Because of the dipole configuration of the background magnetic field, at low and equatorial latitudes the velocity perpendicular to the magnetic field is essentially vertical to the surface of the Earth (see Figure 2a). The positive velocity corresponds to an upward motion of the equatorial ionosphere, the same as those observed during magnetic storms. The first most important feature shown in Figure 2 is that in response to the increases at $t = 120$ s of the antisunward convection imposed at the top boundary of the polar latitudes, the perpendicular velocity on the dayside at all latitudes quickly increases, even at the equator. This resembles the prompt response of the equatorial ionosphere to the solar wind driving force as observed (e.g., Huang et al., 2005; Kelley et al., 2003). However, the start time of the increase is delayed and the delay is height and latitude dependent. Comparing Figures 2a and 2b, we see that the closer to the equator and the lower the altitude, the greater the delay is, indicating the propagation of the perturbation front from the source region in the polar cap to the equator. The latitudinal time delay is smaller at higher altitudes, indicating faster wave speed at higher altitudes. Since the initial state of the ionosphere/thermosphere is not completely steady state, the ion bulk velocities at low latitudes are still gradually increasing before the enhancement of magnetospheric convection. Although the baseline might be affected by such residual flows, the dramatic increase of the velocity, that is, the response of the system seen in the simulation, is reasonable and the overall conclusion will not be qualitatively affected.

In order to drive the ionospheric plasma perturbations, energy and momentum must be provided from some sources. Here we focus on the momentum transfer and leave the discussion of mass and energy transfer in a future publication. In the case of driving source being in the polar cap magnetosphere and ionosphere, the momentum, which is needed to drive the global ionospheric plasma motion and ultimately the neutral motion through ion-neutral collisions, is transferred in the form of rarefaction waves propagating from the polar cap to the equator (Song & Vasyliūnas, 2011). This issue will be further discussed in section 4. The amount of the momentum in unit volume transferred to the low-latitude ionosphere for the velocity component $v_\perp$ perpendicular to the magnetic field alone, say at 0.5° magnetic latitude and 194.01 km, can be estimated by using the difference of $\rho v_\perp$ after (at 132 s) and before (at 127 s) the rapid increase of the velocity: $\Delta\rho v_\perp \approx 8.675 \times 10^{-18}$ g/cm$^3 \times 7,508.0$ cm/s $- 8.675 \times 10^{-18}$ g/cm$^3 \times 6693.0$ cm/s $\approx 7.0 \times 10^{-15}$ g·s^{-1}·cm^{-2}. This amount of momentum equals to the time scale of the velocity increase multiplied by the plasma pressure gradient and Lorentz force $\mathbf{J} \times \mathbf{B}$ according to the plasma momentum equation, where $\mathbf{J}$ and $\mathbf{B}$ are the electric current density and the background magnetic field, respectively. Any mechanisms of the momentum

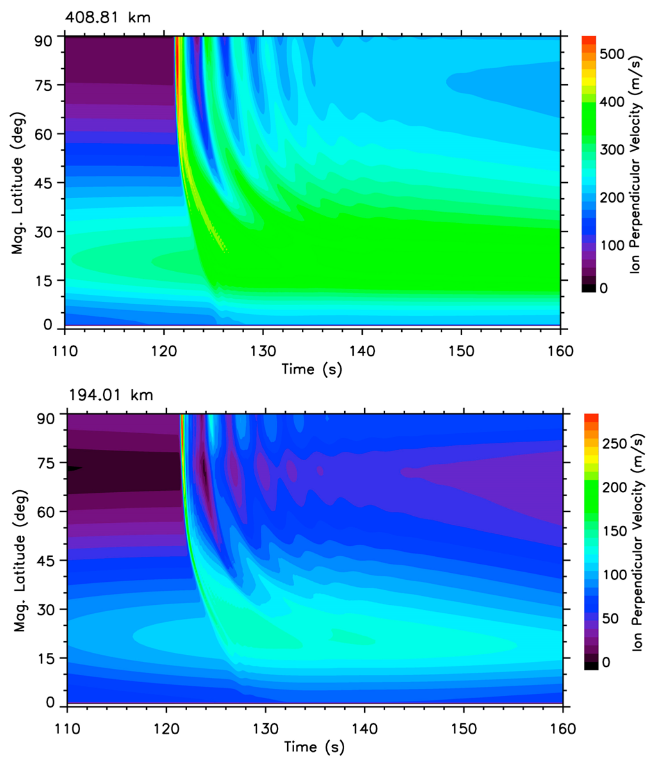

Figure 4. Ion bulk velocity component within the noon-midnight magnetic meridian and perpendicular to the background magnetic field as a function of time and latitude. The upper panel for height of 408.81 km and bottom panel for 194.01 km. The arrival of the velocity perturbations is delayed toward the low latitudes, and the high-frequency oscillation of the perturbations almost completely disappears. The color scale of two panels is different.

transfer from polar region to the equator must provide this amount of momentum density. We will discuss what wave mode in the ionosphere is likely responsible for delivering such amount of momentum later.

The second important feature is the strong oscillations in the ion velocities during the dynamic process before relatively stable situations are established. The enhanced perturbations, or overshoots, can be as large as 50% higher than the stable values eventually reached, a result consistent with the one-dimensional simulations (Song et al., 2009; Tu et al., 2014). The amplitude of oscillations decreases with altitude and latitude. Furthermore, the frequency of oscillations appears also lower at lower heights and latitudes. At the equator and at lower altitudes, the high-frequency oscillations almost completely vanish. The decrease in amplitude and in frequency of the oscillations with altitude and latitude can be understood by the reflection due to changes of the plasma conditions and absorption due to neutral collisions (Song & Vasyliūnas, 2011). When the nonlinear effects are neglected, in an idealized situation, perturbations at the source can be decomposed in Fourier frequency space and each of them propagates independently. The oscillations at a given location and time are a result of the superposition of all incident and reflected waves (Song & Vasyliūnas, 2014; Tu et al., 2011, 2014), from the source region in the entire polar cap via various paths with propagation time delays. The net perturbation is greater when the incidence and reflection are in constructive interference and smaller when the interference is destructive. The interference may substantially complicate the picture because it may change the appearance of time series of observations. Obviously, the magnitude of the velocity is expected to decrease farther away from the source region because less wave power survives the reflection and absorption. Perturbations of higher frequencies are expected to be reflected first because their shorter wavelengths are more sensitive to the background plasma condition changes.

An additional effect to the lower frequency is the inertia loading (Song et al., 2005). At lower frequencies, through collisions, plasma oscillations produce oscillations in a fraction of the neutral population, a process that effectively adds a portion of the neutral mass density to the oscillating magnetic field lines. In turn, this reduces the effective wave propagation speed. The smaller propagation speed further increases the delay time of the response. In the source region (e.g., at 89.5° magnetic latitude), the oscillation demonstrates the situation for magnetospheric perturbation propagating along the field lines down to the ionosphere subjects to reflection that has been studied in the one-dimensional simulations (Song et al., 2009; Tu et al., 2014). Because of the inertia loading effect of the neutrals in the *F* and *E* layers of the ionosphere, the high-frequency waves propagate with diminishing amplitudes, leaving only low frequencies penetrating into the lower altitudes and equator.

In order to have a more comprehensive picture of the global ionospheric response, we show in Figure 3 the time variation and height distribution of the velocity component perpendicular to the background magnetic field at middle and low latitudes. Note that the color scale of two panels is different. Before $t = 120$ s when the driving perturbation at the top boundary of the polar caps is increased, the perpendicular velocity is at its background level, the magnitude is dependent on the altitude and latitude. The arrival of the disturbance enhances the perpendicular velocity quickly above its background level. The greatest increase of the velocity perturbations is seen at the top boundary. The strength of velocity perturbations decreases with the decreasing altitude. The timing of the rapid increase is obviously delayed when moving to lower altitudes and latitudes. All these indicate that the perturbations or in general the ionospheric response seen at low latitudes and low altitudes are associated with the arrival of perturbation fronts propagating from the magnetosphere in the polar latitudes. The enhanced velocity perturbations at any given location are the integration of the wave fronts along all possible paths from the sources distributed along the polar field lines. In addition to modifying the propagation speed, the spatial gradients of the ionosphere/thermosphere densities also produce reflection that serves as a low-pass filter as already demonstrated in Figure 2. It is also

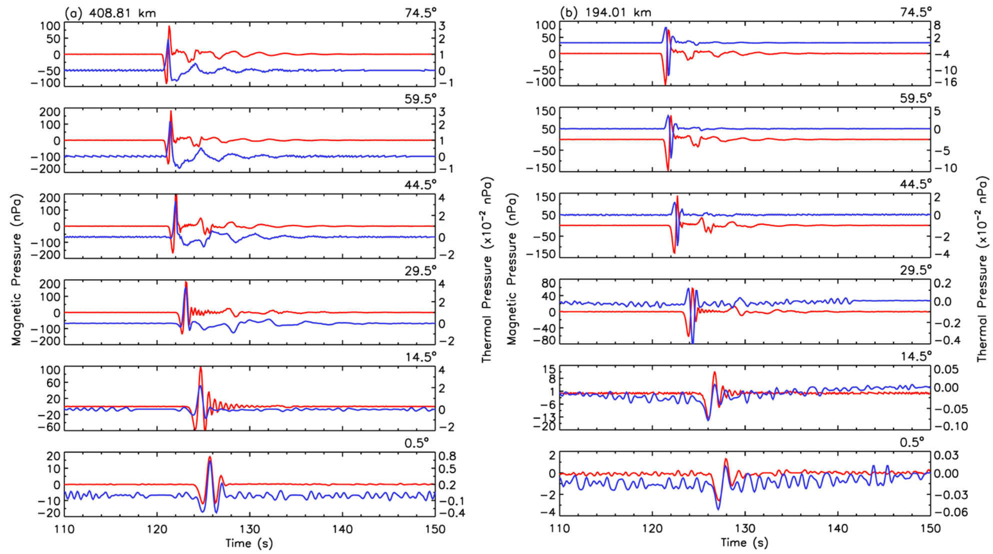

Figure 5. Time variation of the magnetic field (red lines) and plasma thermal pressure (blue lines) for several magnetic altitudes at 408.81 km (a) and 194.01 km (b). The pressures are processed with 1-s running window average, and the averaged values are deducted from the nonaveraged values.

seen that at high heights, the delay at different latitudes is smaller and at heights above 1,500 km the delay is essentially the same. The delay of the wave arrival with respect to latitudes, reflection, and oscillation caused by superposition of the incoming and reflected waves will be further demonstrated in Figure 4.

Another important feature shown in Figure 3 is that the velocity perturbations do not penetrate significantly through the ionosphere below about 150 km, particularly when the oscillation in the velocity perturbations is subsided. Equivalently, the electric field associated with the ion velocity perturbations does not penetrate significantly to the altitudes below about 150 km either.

The low-pass frequency filtering effect is also evident in the perpendicular velocity variations with time and distribution with the latitude, for the topside and *F* region altitudes (Figure 4). The arrival of the wave front at any given altitude is delayed with decreasing latitude. The propagation of the wave from higher latitudes to lower latitudes is clearly shown at both altitudes. Perturbations along different paths may have different time delays to any observation point. Comparing Figure 4 with Figure 3, the features in two panels of Figure 4 are more similar than these in two panels of Figure 3. Combining the feature that the higher the heights, the smaller the delay of velocity increase at different latitudes (see Figure 3), we may infer that the perturbations propagate along paths first from high to low latitudes at altitudes above 1,500 km and then from high to low altitudes (like path B in Figure 7a) is faster than along paths first from high to low altitudes in the polar cap and then from high to low latitudes (like path A in Figure 7a).

For the wave that propagates from the magnetosphere to the high-latitude ionosphere, the source of the perturbation is assumed above 74° in the present simulation. Comparing velocity perturbations at two altitudes, in the polar cap a smaller strength is seen at the lower altitude, indicating substantial damping and reflection of the energy flux from the source along the field. The reflection, on the other hand, may enhance the wave amplitude if the incident and reflected waves are in constructive interference. An example is shown in the lower panel of the Figure 4 for the region above 60° as a narrow enhancement around 122 s. Reflection can also occur associated with the ion density increase toward the equator. Note that the magnitude of velocity perturbations in the equatorial ionosphere at both altitudes after the arrival of the wave fronts is enhanced with change in tens of meters per second, comparable with that observed by the Jicamarca Radar measurements in *F* layer at the equator (see Kelley et al., 2003).

The possible electromagnetic wave modes that carry the perturbations (and thus the energy and momentum) included in the simulation model are the three MHD modes with modification of the collisional effects: shear Alfvén wave and slow- and fast-mode magnetosonic waves (Song & Vasyliūnas, 2014; Tu & Song, 2016). Although the velocity has three components, the dominant velocity perturbations are in the same plane as the background magnetic field (in the present study, the noon-midnight meridian). Because the

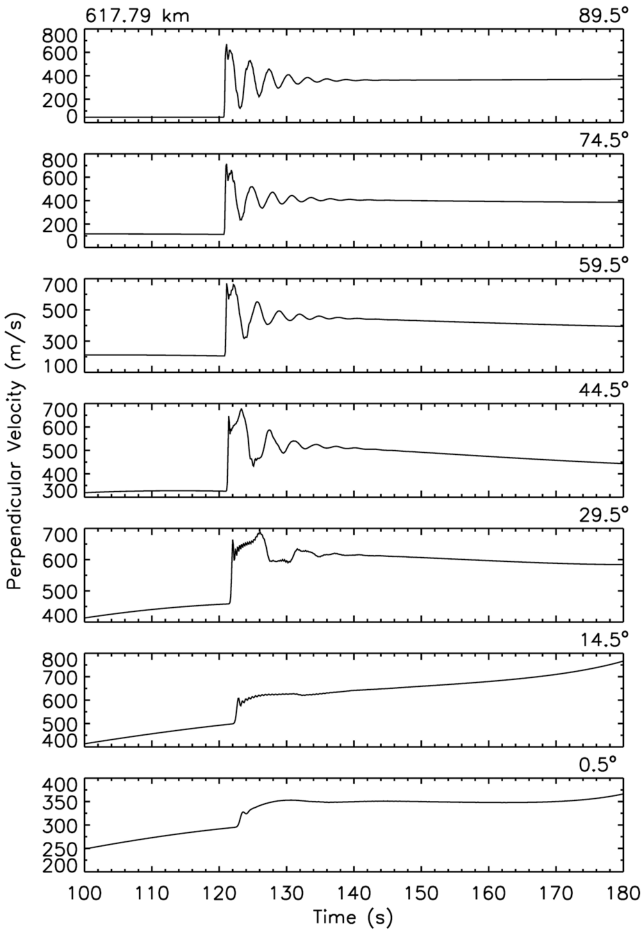

Figure 6. Time variation of $V_\perp$ for several magnetic latitudes at 617.79 km. Positive values represent poleward (at high and middle latitudes) or upward (at low and equatorial latitudes) velocities for the background dipole magnetic field used in the simulation.

propagation direction of interest for high to low latitudes is also in this plane, the modes of interest are fast and slow modes, from the coplanarity theory (Kivelson & Russell, 1985). The diagnostics for the two modes are the phase relation between the magnetic pressure and thermal pressure. When they are in (anti) phase, it is the fast (slow) mode. In order to determine what the wave mode is possibly responsible for the high- to low-latitude coupling, we show in Figure 5 time variations of the perturbation magnetic field pressure (red lines) and plasma thermal pressure (blue lines) at given altitudes of 408.81 km (panel a) and 194.01 km (panel b), respectively. Because the fluctuations of the perturbation magnetic field and thermal pressure are very small in the lower altitudes and lower latitudes compared to the background magnetic field and thermal pressures, respectively, both the magnetic field and thermal pressures have been running averaged over 1 s and then the averages are subtracted from their nonaveraged values. It is shown that the thermal and magnetic pressure perturbations are dominantly out of phase above about 44° but in-phase below this latitude. This in-phase characteristics below 44° latitude shows the first unambiguous evidence that the coupling to the low latitudes is accomplished by the fast magnetosonic waves. The out-of-phase above 44° latitude is somewhat less easy to interpret. Our interpretation is that because the higher latitudes are close to the source region and fast-mode speed is large, greater than 3,000 km/s (see Figure 8), the initial perturbations quickly propagate away, faster than the onset time of 0.5 s for the imposed magnetospheric convection to increase from 200 to 2,000 m/s. After the fast-mode front propagating away, the local equilibrium is quickly reached and forms structures with nearly constant total pressure across them and moving with the flow slowly so that the magnetic pressure is out of phase with the thermal pressure. Note that the hydromagnetic description in which the ionosphere is prescribed as a nonreactive conducting media can not provide such phase relation between the magnetic and thermal pressures.

In the above we have shown that the transmission of the momentum from high to low latitudes is most likely due to fast magnetosonic waves propagating from sources distributed in altitudes in the polar antisunward convection region. The response observed at any given location at low latitude/altitude is the superposition of the waves propagating from various paths. The delay of the response at low latitude and low altitude is caused by limited MHD wave propagation speed. When the wave speed is relatively large, one would observe smaller time delay. This is illustrated in Figure 6 in which the time variation of the perpendicular velocity for multiple latitudes at 617.79 km is displayed. We see that the time delay at all latitudes is within about 2 s because the low plasma density in the topside ionosphere results in relative high MHD wave speeds. Therefore, it is not surprising that one would observe indiscernible delay of the topside equatorial ionosphere response to the magentosphere disturbances imposed on the polar latitude ionosphere. In the supporting information we provide a movie showing time evolution of the perpendicular ion bulk velocity (without running time averaging). The movie clearly displays that the waves propagate in all directions from the source region. The fastest path is from high latitude to equatorial at the top boundary and then downward to lower altitudes. It should be pointed out again there is residual background ionosphere flow at middle to low latitude, resulted from initial state of the ionosphere/thermosphere.

4. Discussion and Conclusion

We have studied the ionosphere from high- to low-latitude response to an enhanced magnetospheric convection at the upper boundary of the polar region using a novel 2.5-D collisional-Hall MHD simulation model. Combining the information provided in Figures 1–6, we show that the energy and momentum needed to drive the dayside global ionospheric responses are transferred from polar to the equatorial ionosphere through collisional MHD waves propagating in the ionosphere. The predominant mechanism for

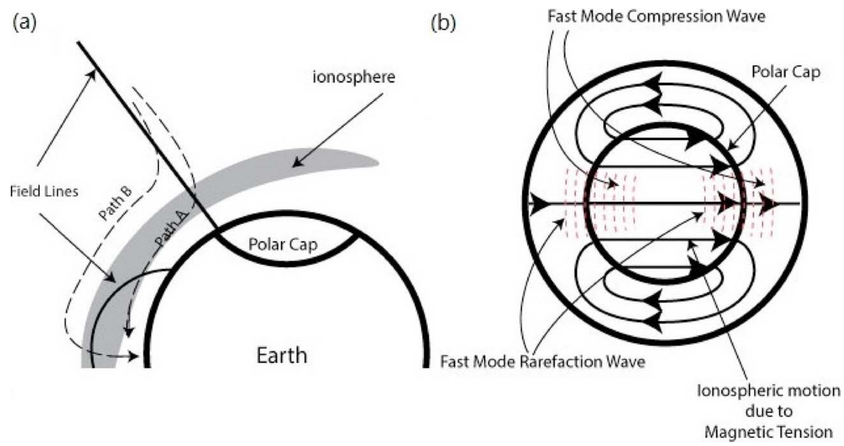

Figure 7. (a) Illustration of two propagation paths of the magnetosonic waves among all possible paths. (b) Schematic demonstration of the ionosphere rarefaction produced by antisunward convection in the polar cap.

high to low-latitude energy and momentum coupling is the fast magnetosonic waves (in a form of rarefaction waves). The physical process can be understood as follow. When the solar wind driver pushes the dayside polar cap magnetosphere-ionosphere to move antisunward, it forms a lower-pressure region immediately on the lower latitude side of the dayside cusp, producing an equatorward pressure gradient, that is, a poleward force. Consequently, the motion produces a lower pressure on its adjacently lower latitude. This low-pressure region continuously propagates to lower and lower latitudes as a rarefaction wave front, as schematically demonstrated in Figure 7(b). The poleward pressure gradient associated with this rarefaction wave and Lorentz force $\mathbf{J} \times \mathbf{B}$ delivers energy and momentum to drive a poleward flow (at middle and high latitudes) or upward flow (at low and equatorial latitudes). The region of poleward (upward flow) expands quickly toward lower and lower latitudes, forming a wave front propagating from high to low latitudes and meanwhile from high to low heights.

The oscillations seen in the simulation are an interesting phenomenon. In theory, it may be produced by oscillations in the source. When the driver is a step function, as we used, the highest frequency of a step function is the Nyquist frequency in the ramp of the driver. If the source is not sustained for the time scale longer than that of interest, the source is effectively a pulse, which carries a lower-frequency cutoff. In this case, it is unlikely that significant momentum can be transferred to the lower latitude in the time scale of interest. Since our driver is sustained with a 0.5-s ramp, there is an intrinsic 1-Hz wave from the source. However, since the period of oscillations at the top is slightly larger than 2 s, it is unlikely to be produced by the Nyquist frequency of the source. It may be a result when the rarefaction perturbations propagate from the polar region to the equatorial and reflect back to form an eigenmode. The speed of fast-mode rarefaction waves at high altitudes is very high. Figure 8 shows Alfvén speed as a function of latitude and altitude for the dayside Northern Hemisphere. The fast-mode wave speed is equal to or higher than the Alfvén speed. For the fast-mode speed of over thousands of kilometers per second and traveling a distance of $\pi R_E/2$, the expected period is in the range of a few seconds. Oscillations produced by different source perturbations and different size of polar cap as well as different top boundary heights remain to be investigated with runs under different settings. Nevertheless, the ionosphere-thermosphere system acts as a low-pass filter system. One may also conjecture that the oscillation is associated with the duct propagation of the Alfvén resonator that may trap hydromagnetic waves between E layer of the ionosphere and the Alfvén velocity minimum at altitude of about 400 km (e.g., Fraser, 1975; Fujita & Tamao, 1988). The movie provided in the supporting information shows that the waves are reflected back and forth between the bottom and upper boundary of the simulation domain in the polar cap regions, which may be a signature of the Alfvén resonator. Further simulations with the upper boundary extending to higher altitude will be used to investigate this possible Alfvén resonator effect. Note that when the ions are driven by the MHD wave to move, they act as transmitters to let waves propagate outside the Alfvén speed minimum instead of completely reflected there.

We have estimated the momentum density required to drive observed equatorial ionosphere upflows. Here we calculate momentum density of an electromagnetic wave propagating in vacuum (Earth's atmosphere basically can be treated as vacuum). Assuming the electric field is 100 mV/m (an over estimation), the instant

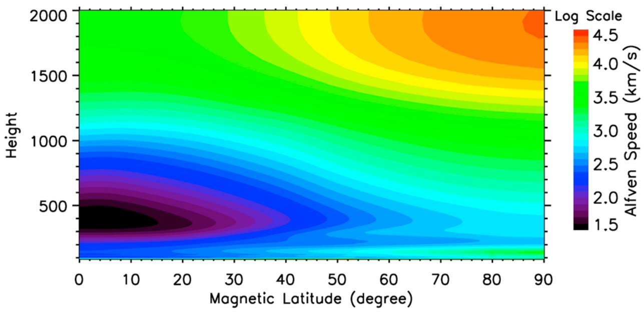

Figure 8. Latitude-altitude distribution of Alfvén speed in the dayside Northern Hemisphere. Note that in the time period simulated, the ion density does not change significantly so that the Alfvén speed is nearly a constant in time.

momentum density will be $\epsilon_0 E^2/c \sim 3\times10^{-19}$ g·s^{-1}·cm^{-2}, at least 4 orders of magnitude smaller than that estimated from the simulation: 7×10^{-15} g·s^{-1}·cm^{-2}. As shown in Figure 3, the perturbation velocity of the plasma does not significantly penetrate below 150 km. Thus, the associated electric field penetrates to below 150 km is far weaker than 100 mV/m, and the amount penetrates into the Earth-ionosphere waveguide is even weaker. Therefore, the electric field transmission through the Earth-ionosphere waveguide (Kikuchi et al., 1978) is not likely the mechanism of the momentum transfer from the high- to low-latitude ionosphere. The MHD waves can carry enough momentum simply because its speed is far less than the speed of light in vacuum.

The simulation results for the first time clearly reveal the MHD wave transmission process of the momentum to the equator during initial prompt response of the ionosphere in terms of the plasma velocity/pressure and magnetic field perturbations, which greatly elucidates our understanding of the underlying physics. A steady state solution of the magnetosphere in 2-D cannot be reached without substantial artificial diffusion. In the present simulation, although after the transit process is passed, the system still evolve slowly. Nevertheless, since the focus of this study is the transit process associated with the M-I coupling and coupling within the ionosphere, the slowly varying process does not invalidate qualitatively the conclusion about the transit process. We only examine short time response of the low/equatorial ionosphere using a nearly step function driver at the top boundary of the polar caps. The longer time scale response from higher upper boundaries, the longer time scale of the input disturbances, and the coupling from the region between the lower boundary and ground is beyond the scope of the present study. The case that the source region is at the equator will be also investigated in the future studies.

The present study focuses on qualitative understanding of physical processes of the momentum transfer through MHD waves. Further simulations will be conducted using more realistic magnetospheric driver, and comparison of the simulation results with ground-based and satellite observations will be performed to quantitatively validate the simulation model. Based on the success of this study, three-dimensional multifluid-collisional-Hall MHD simulations of the global ionosphere/thermosphere using this simulation algorithm combined with the multipoint, multiinstruments observations will unveil the global energy and momentum transmission, which is essential toward building the capability of space weather forecasting.

Acknowledgments
This study was supported by the NSF Grants AGS-1559717 and AGS-1702134 to the University of Massachusetts Lowell. We thank Vytenis Vasyliūnas of Max Planck Institute and Chaosong Huang of Air Force Research Laboratory for valuable discussions. The data from the simulation can be downloaded at the ulcar.uml.edu/downloads.html website.

References

Bilitza, D., Altadill, D., Truhlik, V., Shubin, V., Galkin, I., Reinisch, B., & Huang, X. (2017). International Reference Ionosphere 2016: From ionospheric climate to real-time weather predictions. *Space Weather*, *15*, 418–429. https://doi.org/10.1002/2016SW001593

Borovsky, J. E. (2014). Feedback of the magnetosphere. *Science*, *343*, 1086–1086.

Brambles, O. J., Lotko, W., Zhang, B., Wiltberger, M., Lyon, J., & Strangeway, R. J. (2011). Magnetosphere sawtooth oscillations induced by ionospheric outflow. *Science*, *332*, 1183–1186.

Buonsanto, M. J. (1999). Ionospheric storms—A review. *Space Science Reviews*, *88*, 563–601.

Chi, P. J., Russell, C. T., Raeder, J., Zesta E., Yumoto, K., Kawano, H., et al. (2001). Reply to comment by T. Kikuchi and T. Araki on "Propagation of the preliminary reverse impulse of sudden commencements to low latitudes" *Journal of Geophysical Research*, *107*, A12. https://doi.org/10.1029/2002JA009369

Dungey, J. W. (1961). Interplanetary magnetic field and the auroral zones. *Physical Review Letters*, *6*, 47–48.

Fejer, B. G. (2011). Low latitude ionospheric electrodynamics. *Space Science Reviews*, *158*, 145,166.

Fraser, B. J. (1975). Ionospheric duct propagation and Pc1 pulsation source. *Journal of Geophysical Research*, *80*, 2790–2796.

Fujita, S., & Tamao, T (1988). Duct propagation of hydromagnetic waves in the upper ionosphere: 1. Electromagnetic field disturbances in high latitudes associated with localized incidence of a shear alfvén wave. *Journal of Geophysical Research*, *93*(A12), 14,665–14,673.

Hapgood, M. (2012). Prepare for the coming space weather storm. *Nature*, *484*, 311–313.

Huang, C. S., Foster, J. C., & Kelley, M. C. (2005).Long-duration penetration of the interplanetary electric field to the low-latitude ionosphere during the main phase of magnetic storms. *Journal of Geophysical Research*, *110*, A11309. https://doi.org/10.1029/2005JA011202

Kelley, M. C., Makela, J. J., Chau, J. J., & Nicolls, M. J. (2003). Penetration of the solar wind electric field into the magnetosphere/ionosphere system. *Geophysical Research Letters*, *30*(4), 1158. https://doi.org/10.1029/2002GL016321

Kikuchi, T., Araki, T., Maeda, H., & Maekawa, K. (1978). Transmission of polar electric fields to the equator. *Nature*, *273*, 650–651.

Kim, H., Lessard, M. R., Engebretson, M. J., & Lhr, H. (2010). Ducting characteristics of Pc 1 waves at high latitudes on the ground and in space. *Journal of Geophysical Research*, *115*, A09310. https://doi.org/10.1029/2010JA015323

Kivelson, M. G. (2006). ULF waves from the ionosphere to the outer planets. In K. Takahashi, P. J. Chi, R. E. Denton, & L. Lysak (Eds.), *Magnetospheric waves: Synthesis and new directions*, Geophys Monograph Series (Vol. 169, pp. 11–30). Washington, DC: American Geophysical Union.

Kivelson, M. G., & Russell, C. T. (Eds.) (1985). *Introduction to space physics*. New York: Cambridge University Press.

Kivelson, M. G., & Southwood, D. J (1988). Hydromagnetic waves and ionosphere. *Geophysical Research Letters*, *15*(11), 1271–1274.

Lysak, R. L. (1993). Generalized model of the ionospheric Alfvén resonator. In R. L. Lysak (Ed.), *Auroral plasma dynamics*, Geophys Monogr Series (Vol. 80, pp. 121–128). Washington, DC: American Geophysical Union.

Parker, E. N. (2007). *Conversations on electric and magnetic fields in the Cosmos*. Princeton, NJ: Princeton University Press.

Patel, V. L., & Lagos, P. (1985). Low frequency fluctuations of the electric field in the equatorial ionosphere. *Nature*, *313*, 559–560.

Picone, J. M., Hedin, A. E., Drob, D. P., & Aikin, A. C. (2002). NRLMSISE-00 empirical model of the atmosphere: Statistical comparisons and scientific issues. *Journal of Geophysical Research*, *107*(A12), 1468. https://doi.org/10.1029/2002JA009430

Polyakov, S. V., & Rapoport, V. O. (1981). Ionospheric Alfvé,n resonator. *Geomagnetism and Aeronomy*, *21*(302), 610–614.

Regi, M., De Lauretis, M., Francia, P., & Villante, U. (2014). The propagation of ULF waves from the Earth's foreshock region to ground: The case study of 15 February 2009. *Earth, Planets Space*, *66*, 9. https://doi.org/10.1186/1880-5981-66-43

Richmond, A. D., Maute, A., & Khazanov, G. (2014). Ionospheric electrodynamics modeling. In J. Huba, R. W. Schunk, & G. Khazanov (Eds.), *Modeling the ionosphere-thermosphere system*, Geophysical Monograph Series (Vol. 201, pp. 57–73). Washington, DC: American Geophysical Union.

Robinson, R. M., & Behnke, R. A. (2001). The U.S. National Space Weather Program: A retrospective. In P. Song, J. Singer, & G. Siscoe (Eds.), *Weather, Geophysical Monogr Series* (Vol. 125, pp. 1–10). Washington, DC: American Geophysical Union.

Schunk, R. W., & Nagy, A. F. (2000). *Ionospheres: Physics, plasma physics and chemistry*. New York: Cambridge University Press.

Song, P., & Vasyliūnas, V. M. (2011). How is the ionosphere driven by the magnetosphere. In *IEEE Proceeding of General Assembly and Scientific Symposium 30Th URSI*, Istanbul, Turkey. https://doi.org/10.1109/URSIGASS.2011.6050873

Song, P., & Vasyliūnas, V. M. (2014). Inductive-dynamic coupling of the ionosphere with the thermosphere and the magnetosphere. In J. Huba, R. W. Schunk, & R. W. Khazanov (Eds.), *Modeling the ionosphere-thermosphere system*, Geophys Monograph Series (Vol. 201, pp. 201–215). Washington, DC: American Geophysical Union.

Song, P., Vasyliūnas, V. M., & Ma, L. (2005). Solar wind-magnetosphere-ionosphere coupling: Neutral atmosphere effects on signal propagation. *Journal of Geophysical Research*, *110*, A09309. https://doi.org/10.1029/2005JA011139

Song, P., Vasyliūnas, V. M., & Zhou, X.-Z. (2009). Magnetosphere-ionosphere/thermosphere coupling: Self-consistent solutions for a one-dimensional stratified ionosphere in three-fluid theory. *Journal of Geophysical Research*, *114*, A08213. https://doi.org/10.1029/JA013629

Tu, J., & Song, P. A. (2016). Two-dimensional global simulation of inductive-dynamic magnetosphere-ionosphere coupling. *Journal of Geophysical Research: Space Physics*, *121*, 11,861–11,881. https://doi.org/10.1002/2016JA023393

Tu, J., Song, P., & Reinisch, B. W. (2008). On the concept of penetration electric field. In P. Song, J. Foster, M. Mendillo, & D. Bilitza (Eds.), *Radio sounding and plasma physics, AIP Conference Proceeding* (Vol. 974, pp. 81–85). New York: AIP Publishing.

Tu, J., Song, P., & Vasyliūnas, V. M. (2011). Ionosphere/thermosphere heating determined from dynamic magnetosphere-ionosphere/thermosphere coupling. *Journal of Geophysical Research*, *116*, A09311. https://doi.org/10.1029/2011JA016620

Tu, J., Song, P., & Vasyliūnas, V. M (2014). Inductive-dynamic magnetosphere-ionosphere coupling via MHD waves. *Journal of Geophysical Research: Space Physics*, *119*, 530–547. https://doi.org/10.1002/2013JA018982

Vasyliūnas, V. M. (2001). Electric field and plasma flow: What drives what? *Geophysical Research Letters*, *28*, 2177–2180.

Vasyliūnas, V. M. (2007). The mechanical advantage of the magnetosphere: Solar-wind-related forces in the magnetosphere-ionosphere-Earth system. *Annals of Geophysics*, *25*, 255–269.

Walsh, B. M., Foster, J. C., Erickson, P. J., & Sibeck, D. G. (2014). Simultaneous ground- and spacebased observations of the plasmaspheric plume and reconnection. *Science*, *343*, 1122–1125.

Wright, A. N. (1996). Transfer of magnetosheath momentum and energy to the ionosphere along open field lines. *Journal of Geophysical Research*, *101*(6), 13,169–13,178.

Ziesolleck, C. W. S., & Chamalaun, F. H. (1993). A two-dimensional array study of low-latitude PC 5 geomagnetic pulsations. *Journal of Geophysical Research*, *98*, 13,703–13,713.